A Probabilistic Model for the Scale Effect on Fracture Toughness of Structural Ceramics

Amkee Kim* and Seung-Hoon Nahm**

(Received September 8, 1997)

The fracture toughness of polycrystalline ceramics used to present the scale effect as well as statistical distribution. It is believed that both (scale effect and scatter) must be associated with the heterogeneity of materials. However, no generally accepted theory has been established so far. Using statistical approach, a probabilistic modelling for the fracture toughness which describes the scale effect was attempted in this paper. Weibull distribution of specific fracture energy (SFE) at local area and Griffith criterion are jointly applied to the model. Finally, the fracture toughness scale dependence of ASTM E399 standard specimens was investigated by the newly developed model.

Key Words: Fracture Toughness, Brittle Fracture, Probability, Weibull Distribution, Griffith Criterion, Structural Ceramics, Scale Effect

1. Introduction

Ceramics have been used in many engineering applications such as machinery parts and aerospace structural components mainly due to their excellent high temperature performance as well as wear resistance. The mechanical behavior of ceramics is important when the part is used primarily for carrying a load. Thus, understanding the nature of mechanical behavior of ceramics is essential to alleviate problems against the structural integrity.

One of well known characteristics regarding ceramics is that their strength is very sensitive to the presence of flaws which used to be introduced unpredictablely during fabrication and machining processes, and thus the failure is often not only unexpected but also catastrophic.

The large strength variation of those materials has been conveniently explained by many researchers using the weakest link theory originally proposed by Weibull. (Frendenthal, 1968) This assumes that the failure of the weakest element among all the elements which comprise an isotropic and statistically homogeneous component would cause the whole component to fail. The simplest form of the weakest link theory for brittle material of volume, V, under a uniaxial tension stress, σ, can be written as

$$P_f = 1 - \exp\left[-V\left(\frac{\sigma}{\sigma_o}\right)^m\right] \tag{1}$$

where P_f is the failure probability, σ_o is a material parameter and m is the Weibull modulus. Therefore it is manifested that the scale effect of strength can be explained through the volume, V, in Eq. (1).

As far as the fracture toughness based on linear elastic fracture mechanics (LEFM) of heterogeneous brittle ceramics is concerned, scale dependence as well as scatter often makes it difficult to utilize the fracture toughness as a design parameter. (Bao et al, 1994; Calomino et al., 1992; Chudnovsky et al., 1992; Gurumoorthy et al., 1988; Neville, 1987) Although one intuitively believes that those would be associated with the structural heterogeneity of material, and could be formulated through a distribution of heter-

* Dept. of Mechanical Engineering, Kongju National University 182 Shinkwan-dong, Kongju, Chungnam, 314-701, Korea

** Korea Research Institute of Standards and Science P. O. Box 102 Yusong, Taejon, 305-600, Korea

ogeneity such as Eq. (1), generally accepted theories to describe those phenomena have rarely been found so far.

Indeed, there is a significant difference between the conventional strength which deals with generalized stress and the fracture toughness which deals with concentration of stress and localization of deformation ahead of crack. Thus questions and related formalisms about fracture toughness behavior of heterogeneous brittle ceramics have still been waiting to be resolved.

Recently a probabilistic study on bridging fracture mechanics and weakest link theories for heterogeneous brittle material has been attempted. (Chudnovsky et al., 1987) It is based on a notion of crack formation probability of all possible fracture paths, where the weakest link considerations are employed in modelling of local mechanism for crack advance. Following this notion, the statistics for fracture toughness can be characterized by the probability for a sequence of local crack formations because the fracture toughness should be determined by the global instability condition for a crack.

In this paper, a probabilistic model for the fracture toughness of ceramics was formulated based on the notion of instable crack formation in heterogeneous ceramics, which can describe the scale effect of heterogeneous ceramic on the fracture toughness. In addition, the scale effects on fracture toughness for various type of standard specimens were investigated by the model

2. Probabilistic Model of Crack Formation in Heterogeneous Ceramics

2.1 Basic assumptions for model

The following basic physical assumptions are adopted for a mathematical model of crack formation in heterogeneous ceramics.

1. A random field of micro-inhomogeneities (grain, grain boundaries, inclusion, flaws, etc.) is present in the materials. Thus a crack has to overcome a sequence of random obstacles along its path for the growth.

2. Griffith's criterion is a necessary and sufficient condition for an infinitesimal crack extension: the potential energy released due to the crack advance should exceed the energy required to produce the specific fracture energy (2γ). Thus the micro-inhomogeneity is modelled by a random field of specific fracture energy (γ).

3. The crack is random. This is supported by observations of crack trajectories formed in identical specimens subjected to the same loading, no trajectory coincides, even if it can be overlapped. It suggests that, for a given specimen-loading geometry, there is a set Ω of possible independent crack trajectories, and the actual crack path is selected from Ω by chance.

4. Quasi-static loadings are considered. The dynamic effects such as inertia and reflected elastic waves are neglected.

2.2 Probability of crack formation

Let us consider a two-dimensional ceramic plate subjected to external loading and suppose that the crack tip is at a point $\underline{x}$ on ω_0 (see Fig. 1). Then a probability of crack formation $P_{\omega_0}(\underline{x}, \underline{X})$ is defined as the probability that a crack extends from $\underline{x}$ to another point $\underline{X}$. Multiple experiments on crack extension under macroscopically identical conditions demonstrate that crack trajectories are independent of each other. Thus statistical analysis of the observed crack trajectories allows one to characterize the set Ω of all possible crack trajectories connecting $\underline{x}$ and $\underline{X}$. We, now, assume that only one crack forms along one

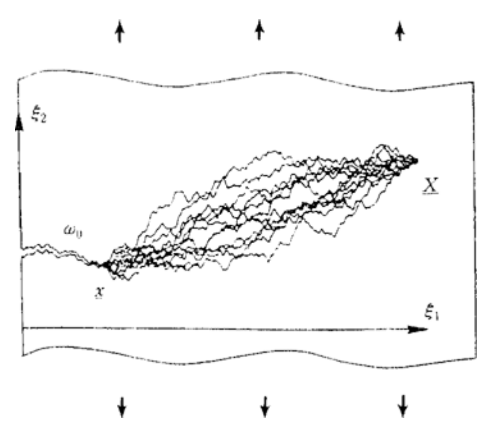

Fig. 1 A visualization of the set Ω of all possible crack paths from crack ω_0 which ends at a point $\underline{X}$.

among those possible trajectories. Then the probability of crack formation $P_{\omega_0}(\underline{x}, \underline{X})$ can be written as

$$P_{\omega_0}(\underline{x}, \underline{X}) = \sum_{\Omega} P_{\omega_0}(\underline{x}, \underline{X}/\omega) P_{\omega_0}[\omega] \quad (2)$$

where $P_{\omega_0}[\omega]$ is the probability that the crack chooses a path ω among all possible trajectories from $\underline{x}$ to $\underline{X}$, and $P_{\omega_0}(\underline{x}, \underline{X}/\omega)$ is the conditional probability that the crack reaches $\underline{X}$ if it is formed along ω. In a continuum based model, the space Ω is uncountable, so we substitute the summation in Eq. (2) by a functional integral

$$P_{\omega_0}(\underline{x}, \underline{X}) = \int_{\Omega} P_{\omega_0}(\underline{x}, \underline{X}/\omega)\, d\mu(\omega) \quad (3)$$

Thus formulation of Eq. (3) requires the following: Selection of an adequate crack trajectory space Ω and the probability measure $d\mu(\omega)$ on Ω, evaluation of the conditional probability $P_{\omega_0}(\underline{x}, \underline{X}/\omega)$ of crack extension along a particular ω and a constructive techniques of computing the integral on the right-hand side of Eq. (3).

In this study, the formulation is proceeded, referring to Chudnovsky' research. (Chudnovsky et al, 1987) We model crack trajectories by lines of an one-dimensional Wiener process $\xi_2 = w(\xi_1)$, $\xi_1 \geq x_1$ in (ξ_1, ξ_2)-plane (for the coordinate system, see Fig. 1). This means that $w(\xi_1)$ is a random process with independent increments, zero drift and a constant gradient $D>0$ of the variance at any point ξ_1 ; D reflects the tendency of crack trajectories to deviate from ξ_1 axis and is experimentally measurable. Thus the space Ω of all possible crack paths connecting $\underline{x}$ and $\underline{X}$ is the space of all continuous functions $w(\xi_1)$ on $x_1 \leq \xi_1 \leq X_1$, satisfying $w(x_1) = x_2$, $w(X_1) = X_2$ and the measure $d\mu(\omega)$ is as follows :

$$\int_{\Omega_{\underline{x},\underline{X}}} d\mu^{(D)}_{\underline{x},\underline{X}}(\omega) = \frac{1}{\sqrt{2\pi D(X_1 - x_1)}} \cdot \exp\left[-\frac{(X_2 - x_2)^2}{2D(X_1 - x_1)}\right] \quad (4)$$

Formulation of the conditional probability $P_{\omega_0}(\underline{x}, \underline{X}/\omega)$ depends on the mechanism of crack growth.

We consider crack formation along ω from $\underline{x}$ to $\underline{X}$ as a sequence of local failures immediately ahead of the current crack tip. Being concerned with brittle crack formation, we adopt Griffith's criterion for infinitesimal crack advance. Namely, the potential energy release rate G must exceed the specific fracture energy 2γ required for fracture surface formation $(G>2\gamma)$. It is further assumed that γ is a random field whose values are independent at distances exceeding a certain small characteristic distance, c. Thus the probability that the criterion of infinitesimal crack advance $(G_C > 2\gamma)$ is satisfied at all points on ω between $\underline{x}$ and $\underline{X}$ is as follows : (see appendix A for the details of derivation of Eq. (5)):

$$P_{\omega_0}(\underline{x}, \underline{X}/\omega) = \exp\left\{-\int_{x_1}^{X_1} \mathrm{Prob}[2\gamma \geq G_{\omega,\omega_0}(\xi_1)] \frac{d\xi}{c}\right\} \quad (5)$$

Here subscripts ω_o, ω of G indicates that G is dependent on the shape of initial crack and the present crack path (see Fig. 1). And, it is assumed that values of γ along crack trajectories represent minimal values of the γ-field, therefore, should provide one of the extreme value distributions (for minima). We choose the following Weibull distribution for the values of γ.

$$F(\gamma) = \begin{cases} 1 - \exp\left[-\left[\dfrac{\gamma - \gamma_{\min}}{\gamma_0}\right]^{\alpha}\right], & \gamma \geq \gamma_{\min} \\ 0, & \gamma < \gamma_{\min} \end{cases} \quad (6)$$

Here, $\gamma_o > 0$, $\alpha > 0$ and $\gamma_{\min} \geq 0$ are scale, shape and minimal value parameters. Combining (3), (4), (5) and (6), the probability of crack formation from $\underline{x}$ to $\underline{X}$ can be described as :

$$P(\underline{x}, \underline{X}) = \int_{\Omega_{x,X}} \exp\left\{-\int_{x_1}^{X_1} \exp\left[-\left[\frac{G_{\omega,\ \omega_0}(\xi_1)/2 - \gamma_{\min}}{\gamma_0}\right]^{\alpha}\right] \frac{d\xi_1}{c}\right\} d\mu^{(D)}_{x,X}(\omega). \quad (7)$$

Since, in case of standard specimens of brittle ceramics, the fracture path is generally formed parallel to the notch direction, D in Eq. (7) can be approximated by zero, and the parameter $\gamma_{\min}$ would also be zero because of the presence of void in materials. Thus, Eq. (7) can be simplified as the following ;

$$P(\underline{x}, \underline{X}) = \exp\left\{-\int_{x_1}^{X_1} \exp\left[-\left[\frac{G_1(\xi_1)/2}{\gamma_0}\right]^{\alpha}\right] \frac{d\xi_1}{c}\right\} \quad (8)$$

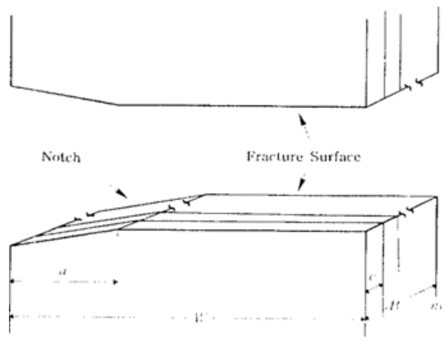

Fig. 2 A specimen with thickness of B is considered as a multilayered specimen composed of n specimens with thickness of c.

3. Probabilistic Model for Fracture Toughness of Ceramics

The fracture toughness, K_c, based on LEFM is evaluated from the stress intensity factor (SIF) at the crack initiation which is corresponding to the maximum test load. Thus the cumulative distribution function of K_c, i.e., $F_{K_c}(K_I)=\mathrm{Pr}ob(K_c<K_I)$, can be defined by the probability that the instable crack continuously propagates from the notch tip(a_N) to the depth of specimen(W) under the load P corresponding to K_I (see Fig. 2). Furthermore, using $G=\frac{K_I^2}{E}$ relationship of LEFM, Eq. (9) for the cumulative distribution function of K_C is obtained from Eq. (8). Here $F_{K_c}(K_I)$ depends on Weibull parameters and the characteristic distance as well as the loading geometries of specimen.

$$F_{K_c}(K_I)=\exp\left\{-\int_{a_N}^{W}\exp\left[-\left[\frac{K_I^2(P,\ \xi_1)/2E}{\gamma_0}\right]^{\alpha}\right]\frac{d\xi_1}{c}\right\} \quad (9)$$

4. Modification of Model for Thickness Effect

Equation (9) for two dimensional ceramic specimen is modified for the specimen with the thickness of B. A specimen with the thickness of B can be considered as a multilayered specimen composed of n specimens with thickness of c depicted in Fig. 2. Thus the event of crack propagation in specimen with the thickness of B from the notch tip, a_N, to the specimen depth, W, is equivalent to the sum of events that the crack in each specimen with the thickness of c propagates from the notch to the depth of specimen. Moreover, suppose that those events are mutually exclusive from each other, then the cumulative distribution function of K_c can be expressed as follows :

$$F_{K_c}(K_I)_{|B}=\prod_{i=1}^{n}\mathrm{Pr}ob\{a\ crack\ formation\ of\ i\text{-}th\ specimen\ from\ a_N\ to\ W\}$$
$$=[F_{K_c}(K_I)]^n=\exp\left\{-\int_{a_N}^{W}\exp\left[-\left[\frac{K_I^2(P,\ \xi_1)/2E}{\gamma_0}\right]^{\alpha}\right]\frac{d\xi_1}{c/n}\right\} \quad (10)$$

It can also be obtained by substituting $c_{eff}=c/n$. Finally, the probability density function of K_c, $f(K_c)_{|B}$, is calculated by differentiating Eq. (10) with respect to K_I as follows :

$$f(K_c)_{|B}=\frac{dF_{K_c}(K_I)_{|B}}{dK_I}\Big|_{K_I=K_c} \quad (11)$$

The mathematical expectation, $\langle K_c\rangle$, and the standard deviation, s, are obtained by the following equations, respectively.

$$\langle K_C\rangle=\int_0^{\infty}K_Cf(K_C)_{|B}dK_C \quad (12)$$

$$s=\sqrt{\int_0^{\infty}K_C^2f(K_C)_{|B}dK_C-\langle K_C\rangle^2} \quad (13)$$

5. Result and Discussion

5.1 Thickness effect on the fracture toughness

In order to verify the model, we compare the mathematical expectation and the variance predicted by the model (Eqs. 12, 13) with experimental data from Gurumoothy's study. (Gurumoorthy et al., 1988) Their data were obtained from the alumina (Al_2O_3) specimens whose geometries are shown in Fig. 3. Here thicknesses of specimens were selected as $B=1.27$ mm, $B=5.10$ mm and $B=19.81$ mm, respectively. The bar marks in Fig. 4 indicate the range of experimental data. The solid line represents the mathematical

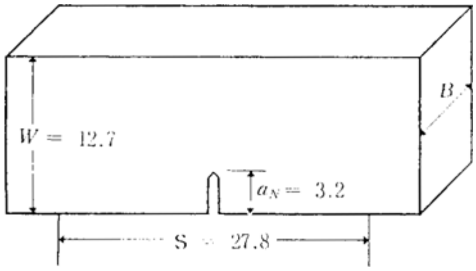

Fig. 3 Three points bend specimen (unit: mm).

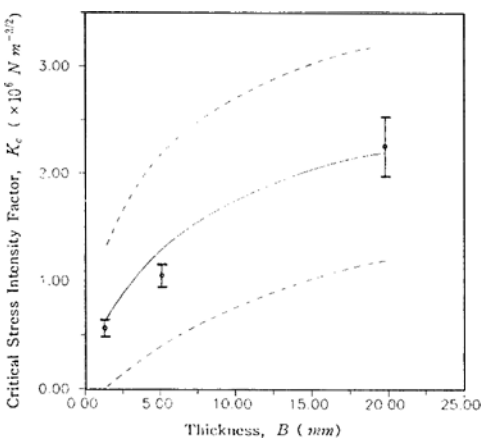

Fig. 4 Toughness variation with thickness.

expectation predicted by the model whose best fitting parameters are $\alpha = 0.25$, $\gamma_0 = 0.02$ J/m^2 and $c = 1$ mm. The dashed lines above and below the solid line represent the 1_S(standard deviation) range of the distribution. As a result, all experimental data fall in the range and close to the mathematical expectation. The tendency of average and variance of experimental data is also in good agreement with those obtained by the model. Particularly the mathematical expectation increases with the increment of specimen thickness.

In general, the increment of mathematical expectation of K_c is not expected in case of metallic materials because the thicker specimen of metallic material provides the more plane strain condition and thus the fracture toughness is reduced. Which may imply that a plane strain fracture toughness can not be utilized as a conservative design parameter in case of ceramics. In other words, the use of the fracture toughness, K_c, evaluated from thick specimen needs caution

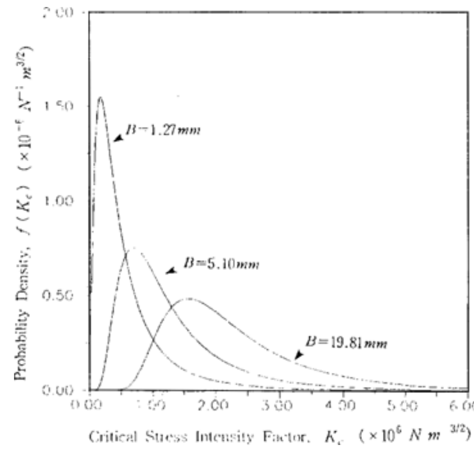

Fig. 5 Probability density distribution of K_c predicted by the model.

when it is applied to the thin structures.

Fig. 5 represents probability density distributions of K_c predicted by the model (Eq. 11) with respect to three points bend specimens whose geometries, Weibull parameters and characteristic distance are same as those employed in Fig. 4.

5.2 Specimen scale effect on the fracture toughness

In order to investigate the scale dependence of K_c by the model, ASTM E399 standard three points bend and compact tension specimens ($B/W = 1/2$) were selected. (ASTM, 1992) Mode I SIF's employed in the model for three points bend and compact tension specimens were evaluated by the equations in appendix B. Figures 6 and 7 represent the scale dependence of the mathematical expectation of K_c with respect to ASTM standard three points bend and compact tension specimens respectively, which are presumably composed of the same material as Gurumoothy et al. tested (i. e., same material parameters are involved). As the depth of specimen, W ($W = 2B$), increases, the mathematical expectation of K_c also increases for both types of specimens. And the difference of initial notch depth ($a_N/W = 0.25$, 0.50, 0.75) provides different values of K_c even with the same depth and thickness of specimen. The specimen containing the shorter initial crack shows relatively the higher K_c value. Moreover, the difference caused by different notch length is

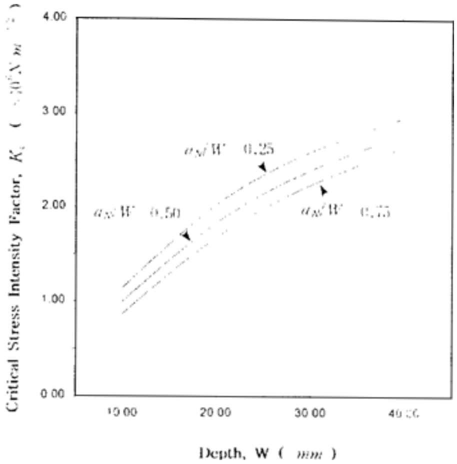

Fig. 6 Scale effect on K_c predicted by the model in case of ASTM E399 three points bend specimen.

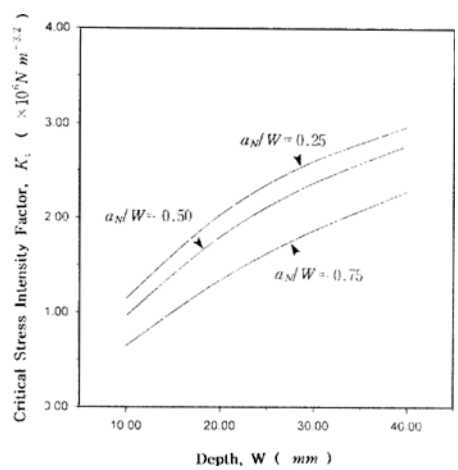

Fig. 7 Scale effect on K_c predicted by the model in case of ASTM E399 compact tension specimen.

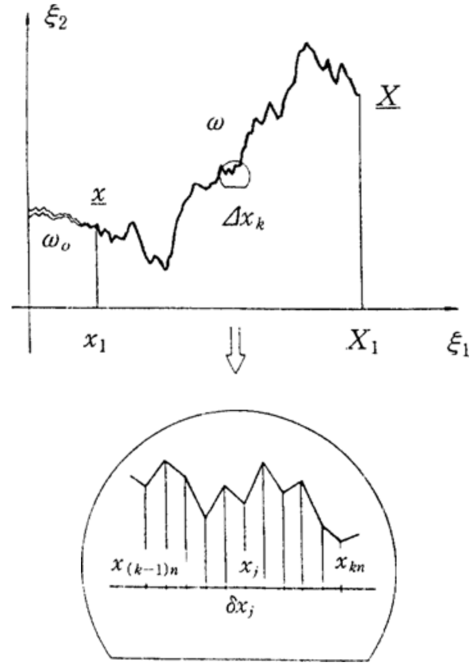

Fig. 8 Discretization of a crack trajectory for the purpose of the probability calculation.

more pronounced in compact tension specimens than in three points bend specimens. Although the variance of K_c is not depicted in the figure, the same tendency is observed.

6. Conclusions

A probabilistic modelling for the fracture toughness of structural ceramics based on bridging fracture mechanics and weakest link theory was attempted. And the scale effect on fracture toughness of ASTM standard specimens was investigated using the model. The conclusions of this study are summarized as follows:

1. A probabilistic model for fracture toughness K_c of heterogeneous ceramics was formulated, which includes Weibull parameters, a characteristic distance as material constants, and geometrical parameters. Thus the scale effect on fracture toughness can be estimated by scaled geometrical parameters in the model.

2. As the depth of specimen $W(W=2B)$ increases, the mathematical expectation and variance of K_c increases for ASTM E399 three points bend and compact tension specimens. The difference of initial notch depth ($a_N/W=0.25$, 0.50, 0.75) provides different results even with the same depth and thickness of specimen. The shorter initial crack provides the higher K_c value. The difference of K_c caused by the different notch length is more pronounced in the compact tension specimen than in the three points bend specimen.

3. Based on Gurumoothy' experimental data, model parameters for alumina are obtained as $a=0.25$, $\gamma_0=0.02$ J/m^2 and $c=1$ mm.

Acknowledgement

The financial support of this work by the Korea Science and Engineering Foundation (Grant No: KOSEF 961-1004-030-1) is gratefully acknowledged.

References

ASTM E399, 1992, Annual Book of ASTM Standards, Vol. 02.02.

Bao, Yiwang, Jin, Zongzhe and Li, Xiaorui, 1994, "Evaluation of K_{IC} Depending on Sample Size for Ceramics," *Engineering Fracture Mechanics*, Vol. 48, No. 1, pp. 85～90.

Calomino, A., Brewer, D., Kim, A. and Chudnovsky, A., 1992, "A Comparative Analysis of Brittle Fracture in Amorphous and Polycrystalline Materials," *Proceedings of Materials Research Society Symposium*, Vol. 279, pp. 165～172.

Chudnovsky, A., Kim, A. and Bosnyak, C. P., 1992, "An Energy Analysis of Crack Initiation and Arrest in Epoxy," *Int. J. of Fracture*, Vol. 55, pp. 209～222.

Chudnovsky, A., and Kunin, B., 1987, "Probabilistic Model of Brittle Crack Formation," *Journal of Applied Physics*, Vol. 62, No. 10, pp. 4124～4129.

Duan, K., Mai, Y. -M. and Cotterell, B. 1995, "R-Curve Effect on Strength and Reliability of Toughened Ceramic Materials," *Journal of Materials Science*, Vol. 30, pp. 1405～1408.

Frendenthal, A. M., 1968 "Statistical Approach to Brittle Fracture," *Fracture an Advanced Treatise*, Vol. 2, Academic Press, pp. 591～619.

Gurumoorthy, B., Kircher, H. O. K., Prinz, F. B. and Sinclair, G. B., 1988, "Thickness Effects May Not Do What You Think Do," *Engineering Fracture Mechanics*, Vol. 29, No. 6, pp. 637～640.

Matsuo, Y., Kitakami, K. and Kimura, S., 1987, "Crack Size and Strength Distribution of Structural Ceramics After Non-Destructive Inspection," *Journal of Materials Science*, Vol. 22, pp. 2253～2256.

Neville, D. J., 1987, "The Non-Conservatism of the Weibull Function when Applied to the Statistics of Fracture Toughness," *Int. J. of Fracture*, Vol. 34, pp. 309～315.

Appendix A

● **Derivation of Eq. (5)**

We subdivide the interval $x_1 < \xi_1 \le X_1$ into m equal portions, $\Delta\xi_k$, whose length $\Delta\xi$ is small enough so that $G_{\omega,\omega_0}(\xi)$ can be considered constant over each $\Delta\xi_k$. At the same time, we assume that $\Delta\xi$ is much greater than the characteristic distance of c, $\Delta\xi \gg c$. Let us further split each $\Delta\xi_k$ into $n(=\Delta\xi_k/c)$ subintervals $\delta\xi_j$, $(k-1)n < j \le kn$, of length c (see Fig. 8) and consider γ to be constant over each $\delta\xi_j$. Thus, the interval $x_1 < \xi_1 \le X_1$ is subdivided into $m \times n$ subintervals $\delta\xi_j$.

Crack formation between x_1 and X_1 means failure over all $\delta\xi_j$'s. According to the energy criterion of local failure, the failure over $\delta\xi_j$ occurs if the released potential energy $\Delta\Pi_j$ is greater than the energy required for new crack surface formation $\Delta\Pi_j > 2\gamma\delta\xi_j$. Thus,

$$P_{\omega_0}(\underline{x}, \underline{X}/\omega) = \mathrm{Pr}ob\left[\bigcap_{j=1}^{mn}(\Delta\Pi_j > 2\gamma_j\delta\xi_j)\right] \tag{A.1}$$

To evaluate the probability, we consider crack formation as an ordered sequence of local failures. Therefore, it is convenient to represent $P_{\omega_0}(\underline{x}, \underline{X}/\omega)$ as the following product of conditional probabilities :

$$P_{\omega_0}(\underline{x}, \underline{X}/\omega) = \prod_{j=1}^{mn}\mathrm{Pr}ob\left[\Delta\Pi_j > 2\gamma_j\delta\xi_j \,\Big|\, \bigcap_{i=1}^{j-1}(\Delta\Pi_i > 2\gamma_i\delta\xi_i)\right] \tag{A. 2}$$

The potential energy released at the jth step under the condition that all preceding elements failed can be evaluated through the energy release rate $G(\xi) = G_{\omega,\omega_0}(\xi)$:

$$\Delta\Pi_j = G(\xi_j)\,\delta\xi_j \tag{A. 3}$$

Thus, equation (A. 2) becomes

$$P_{\omega_0}(\underline{x}, \underline{X}/\omega) = \prod_{j=1}^{mn}\mathrm{Pr}ob[G(\xi_j) > 2\gamma_j]$$

$$=\prod_{k=1}^{m}\prod_{j=(k-1)n+1}^{kn}\mathrm{Pr}ob[G(\xi_j)>2\gamma_j] \tag{A. 4}$$

where the inner product represents the conditional probability of failure over $\Delta\xi_k$. According to the choice of small $\Delta\xi$, $G(\xi)$ is approximately constant over each $\Delta\xi_k$, *i. e.*, for a given k, all the values $G(\xi_j)$ in the inner product in Eq. (A. 4) can be substituted by the same value $G(\xi_{kn})$. Also, γ_j's are independent random variables, which have the same Weibull distribution. We conclude that the probabilities $\mathrm{Pr}ob[G(\xi_j)>2\gamma_j]$ in Eq. (A. 4) are all equal to $\mathrm{Pr}ob[G(\xi_{kn})>2\gamma]$ for a given k. Because the opposite event $\mathrm{Pr}ob[G(\xi_{kn})>2\gamma]=1-\mathrm{Pr}ob[2\gamma\geq G(\xi_{kn})]$ for each of the $n=\Delta\xi/c$ factors, Eq. (A. 4) is summarized as follows :

$$P_{\omega_0}(\underline{x}, \underline{X}/\omega)=\prod_{k=1}^{m}[1-\mathrm{Pr}ob[2\gamma\geq G(\xi_{kn})]]^{\Delta\xi/c} \tag{A. 5}$$

Assuming that $\mathrm{Pr}ob[2\gamma\geq G(\xi_{kn})]$ is small, and using $(1-\xi)^n\simeq\exp(-n\varepsilon)$ where ε small, we rewrite Eq. (A. 5) as follows:

$$P_{\omega_0}(\underline{x}, \underline{X}/\omega)\simeq\exp\left(-\sum_{k=1}^{m}\mathrm{Pr}ob[2\gamma\geq G(\xi_{kn})]\frac{\Delta\xi}{c}\right) \tag{A. 6}$$

Substituting the above summation with integration, Eq. (5) is finally obtained.

Appendix B

● **Mode I stress intensity factor for three points bend specimen**

$$K_I=(PS/BW^{3/2})\cdot f(a/W) \tag{B. 1}$$

where:

$$f(a/W)=\frac{3(a/W)^{1/2}[1.990-(a/W)(1-a/W)}{2(1+2a/W)(1-a/W)^{3/2}}\;\underline{(2.15-3.93a/W+2.7a^2/W^2)]}$$

where:

P=load, B=specimen thickness, S=span, W=specimen depth, a=crack length

● **Mode I stress intensity factor for compact tension specimen**

$$K_I=(P/BW^{1/2})\cdot f(a/W) \tag{B. 2}$$

where:

$$f(a/W)=\frac{(2+a/W)(0.886+4.64a/W-13.32a^2/}{(1-a/W)^{3/2}}\;\underline{W^2+14.72a^3/W^3-5.6a^4/W^4)}$$

where:

P=load, B=specimen thickness, W=specimen depth, a=crack length